Received: 12 October 2017 | Accepted: 9 January 2018
DOI: 10.1002/jcp.26482

FROM THE BENCH

WILEY Journal of Cellular Physiology

Haplo-insufficiency of Bcl2-associated athanogene 3 in mice results in progressive left ventricular dysfunction, β-adrenergic insensitivity, and increased apoptosis

Valerie D. Myers[1] | Dhanendra Tomar[2] | Muniswamy Madesh[2] | JuFang Wang[2] | Jianliang Song[2] | Xue-Qian Zhang[2] | Manish K. Gupta[3] | Farzaneh G. Tahrir[3] | Jennifer Gordon[3] | Joseph M. McClung[4] | Christopher D. Kontos[5] | Kamel Khalili[3] | Joseph Y. Cheung[1,2] | Arthur M. Feldman[1]

[1] Department of Medicine, Lewis Katz School of Medicine at Philadelphia, Philadelphia, Pennsylvania

[2] Center for Translational Medicine, Lewis Katz School of Medicine at Temple University, Philadelphia, Pennsylvania

[3] Department of Neuroscience, Lewis Katz School of Medicine at Temple University, Philadelphia, Pennsylvania

[4] Department of Physiology, Brody School of Medicine, East Carolina University, Greeneville, North Carolina

[5] Division of Cardiology, Department of Medicine, Duke University Medical Center, Durham, North Carolina

Correspondence
Arthur M. Feldman, Departmentof Medicine, Lewis Katz School of Medicine at Philadelphia, 3401 N. Broad Street, Suite 942, Philadelphia, PA 19140.
Email: arthur.feldman@tuhs.temple.edu

Funding information
National Heart, Lung, and Blood Institute, Grant numbers: HL123093, HL58672, HL74854, HL91799

Bcl2-associated athanogene 3 (BAG3) is a 575 amino acid protein that is found predominantly in the heart, skeletal muscle, and many cancers. Deletions and truncations in BAG3 that result in haplo-insufficiency have been associated with the development of dilated cardiomyopathy. To study the cellular and molecular events attributable to BAG3 haplo-insufficiency we generated a mouse in which one allele of BAG3 was flanked by loxP recombination sites ($BAG3^{fl/+}$). Mice were crossed with α-MHC-Cre mice in order to generate mice with cardiac-specific haplo-insufficiency ($cBAG3^{+/-}$) and underwent bi–weekly echocardiography to assess their cardiac phenotype. By 10 weeks of age, $cBAG3^{+/-}$ mice demonstrated increased heart size and diminished left ventricular ejection fraction when compared with non-transgenic littermates ($Cre^{-/-}BAG3^{fl/+}$). Contractility in adult myocytes isolated from $cBAG3^{+/-}$ mice were similar to those isolated from control mice at baseline, but showed a significantly decreased response to adrenergic stimulation. Intracellular calcium ($[Ca^{2+}]_i$) transient amplitudes in myocytes isolated from $cBAG3^{+/-}$ mice were also similar to myocytes isolated from control mice at baseline but were significantly lower than myocytes from control mice in their response to isoproterenol. BAG3 haplo-insufficiency was also associated with decreased autophagy flux and increased apoptosis. Taken together, these results suggest that mice in which BAG3 has been deleted from a single allele provide a model that mirrors the biology seen in patients with heart failure and BAG3 haplo-insufficiency.

KEYWORDS
BAG3, cardiomyopathy (DCM), genetic mutation, haplo-insufficiency

Valerie D. Myers submitted in partial fulfillment of the PhD degree.

1 | INTRODUCTION

Bcl2-associated athanogene 3 (BAG3) is a 575 amino acid protein that is highly conserved in nature (Behl, 2016). Expressed predominantly in the heart, the skeletal muscle, and in many cancers, BAG3 has pleotropic effects in the cell owing to the presence of multiple protein–protein binding domains. For example, it inhibits apoptosis by binding to Bcl2, supports protein quality control (PQC) by serving as a co-chaperone with the heat shock proteins, tethers actin filaments to the Z-disc and facilitates adrenergic responsiveness by coupling the β1-adrenergic receptor and the L-type Ca^{2+} channel (Behl, 2016).

In 2009, Selcen described three children with severe myofibrillar myopathy, skeletal muscle weakness, giant axon disease, and a hypertrophic/restrictive cardiomyopathy that was associated with a non-synonymous single nucleotide polymorphism that resulted in a shift from a proline to a leucine at position 209 (Pro209Leu) (Selcen et al., 2009). Subsequent to the identification of the hypertrophic phenotype, (Norton et al., 2011) identified a family with a dilated cardiomyopathy in the absence of skeletal muscle or neurologic disease that was associated with a large deletion in BAG3. Studies have now identified deletions, truncations and some non-synonymous SNPs as causative in both familial and sporadic cases of dilated cardiomyopathy (Arimura, Ishikawa, Nunoda, Kawai, & Kimura, 2011; Chami et al., 2014; Feldman et al., 2014; Franaszczyk et al., 2014; Toro et al., 2016; Villard et al., 2011) and can result in BAG3 haplo-insufficiency (Feldman et al., 2014; Toro et al., 2016). In fact, investigators recently posited that BAG3 is a major cardiomyopathy locus (Franaszczyk et al., 2014).

Unfortunately, there is a paucity of information regarding the mechanisms that regulate BAG3 function and it's signaling due in part to the absence of viable animal models. Homma reported that mice with homozygous deletion of BAG3 developed a severe non-inflammatory myopathy in both the cardiac and skeletal muscle that resulted in death by 4 weeks of age (Homma et al., 2006). However, mice with heterozygous deletion of BAG3 had a normal phenotype. (Fang et al., 2017) recently mitigated the early lethality of homozygous BAG3 disruption by introducing a transgene that was restricted to the myocardium. The resultant progeny had diminished LV function and decreased autophagy flux, but no cardiac BAG3. They found a similar phenotype in mice in which a non-synonymous single nucleotide polymorphism (SNP) found in humans was knocked-in to both alleles; however, BAG3 levels were normal. The present study was undertaken to create a mouse with heterozygous deletion of BAG3, haplo-insufficiency and LV dysfunction in order to mirror the more common phenotype seen in individuals with a BAG3 deletion or truncation.

2 | METHODS

2.1 | Animal protocols and generation of BAG3 haplo-insufficient mice

All experiments were performed according to the National Institutes of Health Guide for the Care and Use of Laboratory Animals and were approved by the Temple University Institutional Animal Care and Use Committee (ACUP#4380). Because the effects of female hormones on BAG3 expression and function have not been defined, male mice were used in all studies. The background for all mice was C57BL/6.

The strategy for obtaining mice with deletion of BAG3 is found in Figure 1. *BAG3* (HEPD0556_7_B06) mice were obtained from the

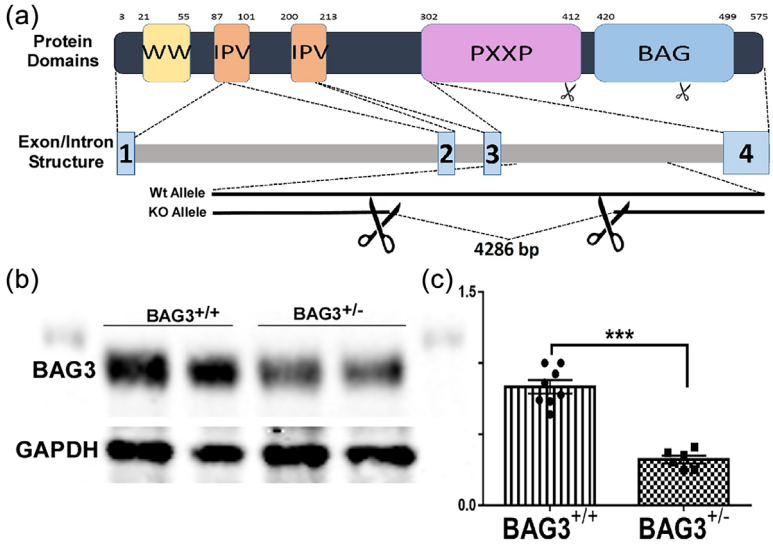

FIGURE 1 Generation of BAG3 haplo-insufficient mouse. (a) A schematic of generation of heterozygous BAG3 knockout mice using recombination between LoxP sites on the BAG3 gene. Numbers on protein cartoon indicate amino acid positon and numbers 1–4 on transcript indicate intron boundaries. (b) Representative western blot of BAG3 levels in both $cBAG3^{+/+}$ and $cBAG3^{+/-}$ mice with glyceraldehyde 3-phosphate dehydrogenase (GAPDH) as the housekeeping protein. (c) Graph showing quantification of BAG3 levels in $cBAG3^{+/+}$ ($n = 8$) and $cBAG3^{+/-}$ ($n = 6$) mice. *** $p < 0.0001$

MRCHarwell which distributes these mice on behalf of the European Mouse Mutant Archive (www.infrafrontier.eu). The MRC-Harwell is also a member of the International Mouse Phenotyping Consortium (IMPC) which funded the generation of the BAG3 floxed mice. Funding and associated primary phenotypic information may be found at www.mousephenotype.org Details of the alleles have been previously published (Bradley et al., 2012; Pettitt et al., 2009; Skarnes et al., 2011). Gene targeting produced a "knockout first" allele with both a PGK-neomycin cassette and a LacZ reporter gene. *loxP* sites flank the promoter/neomycin cassette and were removed by action of cre recombinase, thereby 'knocking out' *BAG3* (Agah et al., 1997). BAG3 single allele floxed ($BAG3^{fl/+}$) mice were crossed with αMHC-Cre mice (Agah et al., 1997) leading to cardiac restricted heterozygous knockdown of *BAG3*. These mice are designated as $cBAG3^{+/-}$ mice. Non-transgenic littermate controls had the genotype $Cre^{-/-}$ $BAG3^{fl/+}$ and are designated as $cBAG3^{+/+}$. Genotyping of mice was done using gel based genotyping on DNA extracted from tails with primers for a WT band (F: TCTGAAGATGCACAGGGGTG, R: TGAGCGGCACTTTAAGGTTT) and primers for a floxed allele (F: TCTGAAGATGCACAGGGGTG, R: GAACTTCGGAATAGGAACTTCG) with the resulting WT band migrating at 300 base pairs and the floxed allele at 139 base pairs.

2.2 | Tissue handling

Mice were weighed, deeply anesthetized with isoflurane, and an incision was made in the abdomen. The inferior vena cava was cannulated, and 30 mmol/L KCl in an isotonic and pH buffered solution was rapidly infused. The heart was then excised, weighed, and rinsed in ice-cold 30 mmol/L KCl. Small portions of the left ventricular free wall were removed and placed in ice–cold 10% neutral buffered formalin and the remaining heart tissue was flash-frozen in liquid nitrogen and stored at −70 °C for subsequent analysis. The tibia was exposed and measured.

2.3 | Echocardiography

Global LV function was evaluated in all mice after light sedation (2% isoflurane) using a VisualSonics Vevo 2100 imaging system and a MS550D scan head (Miami, FL) as described previously (Tilley et al., 2014). The left ventricular ejection fraction (LVEF) was calculated using the formula EF% = [(LVEDV − LVESV)/LVEDV] × 100; where LVEDV and LVESV are left ventricular end-diastolic volume and left ventricular end-systolic volume, respectively. Fractional shortening (FS) was calculated as FS% = [(LVEDD − LVESD)/LVEDD] × 100.], where LVEDD and LVESD are left ventricular end-diastolic dimension and end-systolic dimension, respectively.

2.4 | Isolation of adult cardiac myocytes, single cell contractility, and Ca^{2+} transients

Cardiac myocytes were isolated from the septum and LV free wall of $cBAG3^{+/-}$ or $cBAG3^{+/+}$ mice (10–12 weeks old) as previously described (Zhou et al., 2000) and plated on laminin-coated glass coverslips (Tucker et al., 2006). Coverslips were then mounted in a Dvorak-Stotler chamber and bathed in fresh media before measurements.

Measurements of contraction and $[Ca^{2+}]_i$ in adult cardiac myocytes were obtained as described previously (Feldman et al., 2016). In brief, myocyte contraction was recorded using a charge-coupled device video camera and myocyte motion was analyzed offline with an edge detection algorithm. (Song et al., 2008, 2012; Tucker et al., 2006; Wang et al., 2009, 2010, 2011). For measurement of calcium transients, Fura-2 loaded myocytes adherent to laminin-coated coverslips were incubated in buffer (1.8 mM $[Ca^{2+}]_o$) and field stimulated to contract (2 Hz; 37 °C). Myocytes were exposed to excitation light (360 and 380 nm) only during data acquisition. Epifluorescence (510 nm) was measured in steady-state twitches both before and after addition of isoproterenol (Iso; 1 μM) (Song et al., 2008; Song et al., 2012; Wang et al., 2010; Wang et al., 2009 Wang et al., 2011).

2.5 | Immunoblotting

Immunoblots were performed as described previously (Su et al., 2016). In brief, snap frozen left ventricles were lysed in buffer, and homogenized in a Bullet Blender. Twenty-five Microgram of reduced protein lysates were run on SDS-PAGE gels and transferred to Odyssey nitrocellulose membranes for blotting. Blots were then incubated with a primary antibody and secondary antibodies prior to scanning with an Odyssey scanner and quantification using Image Studio software. The primary antibodies were BAG3 (Cat. # 10599-1-AP, Protein Tech, Rosemont, IL) and GAPDH (Cat.# sc-137179, Santa Cruz Biotechnology, Dallas TX). Secondary antibodies were goat anti-mouse IRDye 800 (Cat. #926-32210; LiCor Biosciences, Lincoln, NE) and IRDye 680 goat anti-rabbit (Cat. #926-68071; Licor Biosciences, Lincoln, NE).

2.6 | Measurement of autophagy flux

Microtubule-associated protein 1A/1B-light chain 3 (LC3) is a soluble protein found ubiquitously in mammalian cells. During autophagy, LC3-1 is conjugated to phosphatidylethanolamine to form LC3-phophatidylethanolamine conjugate (LC3-II) and then is recruited to the autophagasome membrane. When the autophagasome fuses with a lysosome to form an autolysosome, the LC3-II within the autophagalysosome is degraded. Thus, the loss of LC3-II is proportional to the flux of the autophagic complex (Tanida, Ueno, & Kominami, 2008). Because autophagy is ongoing, the measurement of LC3 levels at any time point may not accurately represent actual flux. The addition of bafilomycin A1; however, blocks the fusion of the lysosome and the autophagasome thereby attenuating LC3 lysis. Increased levels of LC3 in the presence of bafilomycin A1 as compared with levels in the absence of bafilomycin suggests that flux is active whereas a lack of change represents a diminution in autophagy flux (Capasso et al., 2015).

Two techniques are available for measuring LC3 levels. First, an adenovirus expressing RFP-GFP-LC3 was constructed as previously described (Su et al., 2016). Isolated adult myocytes from cBAG3$^{+/-}$ and Cre$^{-/-}$BAG3$^{fl/+}$ controls were infected after isolation with Adv-RFP-GFP-LC3 or Adv-null. Confocal imaging was then performed 48 hr later as described in detail previously (mRFP −red–594 nm ex, 667 nm em: GFP–green–488 nm ex, 543 nm em) (Su et al., 2016). Experiments were performed with and without Bafilomycin A1. The puncta of 10–14 cells in each condition from three separate isolations were counted after obtaining digital images. When a lysosome fuses with the autophagasome to form an autophagolysosome, the increased acidity in the resulting autophagalysosome quenches the fluorescence of the GFP signal (green) resulting in predominantly red puncta in the autophagalysosome. As noted above, if autophagy flux is active, and autophagasome and lysosome fusion is inhibited by Bafilomycin A1, the number of puncta in both the autophagalysosomes and in the cytoplasm (yellow) increases because the LC3B-BAG3-protein complexes are not degraded in the autophagalysosome (Klionsky et al., 2016; Ma et al., 2012).

We next corroborated the measurement of autophagy flux in a separate group of experiments, Isolated adult myocytes were plated on six-well plates in the same medium as used for contractility experiments detailed above. Cells were treated for two hours with 50nM bafilomycin A1, lysed in RIPA buffer, vortexed on ice, and spun at 13,000*g* for 6 min at 4 °C. The supernatant was removed and protein concentrations were measured as described previously (Su et al., 2016). We then loaded 15 μg of protein onto an SDS page gel (4–12%) and blotted using primary and secondary antibodies as described above (Immunoblotting). Levels of LC3I and LC3II were then quantified.

2.7 | Measurement of apoptosis

Apoptosis was measured in cBAG3$^{+/-}$ and cBAG3$^{+/+}$ cells using a Detection Kit (Abcam, Cambridge, UK #ab176750) according to manufacturer's instructions. In brief, cells were stained with a red sensor that identifies apoptotic cells by detecting the shift in phosphatidylserine from the inner to the outer surface of the myocyte. (Ex/Em = 630/660 nm). Next, a membrane-impermeable DNA Nuclear Green DCS1 (Ex/Em = 490/525 nm) was used to demonstrate late stage apoptosis(cells both red and green) and necrosis (green alone). Cells were also stained with CytoCalcein Violet 450 (Ex/Em = 405/450 nm) in order to identify living cells (blue) with intact sarcolemma. Live cells were imaged on a Zeiss 510 confocal microscope. The number of viable cells per field was counted by an investigator blinded to the experimental group of each sample to avoid bias and a minimum of 100 cells were counted per group. Results are presented as percentage of apoptotic cells per total cells counted.

2.8 | Statistical analysis

Data are presented as means ± SEM for continuous variables. One-way ANOVA with Tukey multiple comparisons adjustments were used to assess differences across the investigational groups. A Two-way ANOVA was also used for autophagy flux analysis and analysis of $[Ca2+]_i$ transient and contraction amplitudes as a function of group and Isoproterenol. Data was analyzed using Graph pad Prizm 6. A $p < 0.05$ was considered statistically significant.

3 | RESULTS

3.1 | Cardiac specific and heterozygous deletion of BAG3 results in haplo-insufficiency

When heterozygous floxed mice were crossed with the α-MHC driven Cre mice,(Figure 1a) the resulting progeny had haplo-insufficiency of BAG3 as seen in the Western blot in Figures 1b and a 51% ($p < 0.0001$) reduction in BAG3 levels when compared with non-transgenic littermate controls (Figure 1c).

3.2 | BAG3 haplo-insufficiency causes left ventricular dysfunction by 10 weeks of age.

Haplo-insufficiency of BAG3 had no effect on echocardiographic measures of LV function at 4 or 8 weeks after birth. (Figures 2a and 2b) However, by 10 weeks of age there was a significant decrease in EF (62.79 ± 6.4 vs 44.53 ± 4.0; $p < 0.0001$) and FS (34.48 ± 4.9 vs 22.05 ± 2.3; $p < 0.001$) in cBAG3$^{+/-}$ mice when compared with non-transgenic littermate controls. The decrease in LV function in the cBAG3$^{+/-}$ mice was sustained as both the ejection fraction (75.26 ± 2.7 vs 43.44 ± 8.9; p = 0.004) and fractional shortening (43.30 ± 2.7 vs 22.89 ± 4.0; p = 0.004) were significantly decreased at 12 weeks. There was also an increase in left ventricular internal systolic dimension (LVIDs) at 12 weeks (1.95 ± 0.04 mm in cBAG3$^{+/+}$ mice vs 3.12 ± 0.2 mm in cBAG3$^{+/-}$ p = 0.01) and left ventricular systolic volume (LV Vol s) between cBAG3$^{+/+}$ and cBAG3$^{+/-}$ mice at 12 weeks (12.20 ± 0.6 μl – cBAG3$^{+/+}$ mice vs 39.83 ± 6.9 μl – cBAG3$^{+/-}$; $p = 0.01$). Other echocardiographic parameters such as cardiac output, LVIDd, LVPWd, LVPWs, LV vol d, and HR were not significantly different between groups at 12 weeks.

3.3 | Single cell contractility and Ca flux are diminished in the presence of isoproterenol

As seen in Table 1, contractility (% cell shortening) in adult myocytes isolated from 10 to 12 weeks old cBAG3$^{+/-}$ mice did not differ from that seen in myocytes isolated from cBAG3$^{+/+}$ control mice. By contrast, in the presence of isoproterenol (1 μM), single cell contractility was significantly ($p < 0.046$) lower in cBAG3$^{+/-}$ mice with haplo-insufficiency then in myocytes isolated from cBAG3$^{+/+}$ control mice. Similarly, $[Ca^{2+}]_i$ transient amplitudes did not differ between cBAG3$^{+/+}$ and cBAG3^{+-} mice at baseline but were significantly lower ($p < 0.0001$) in myocytes isolated from cBAG3$^{+/-}$ mice in the presence of isoproterenol suggestingBAG3 either modulates β-adrenergic responsiveness of L-type Ca^{2+} channels therby limiting Ca^{2+} influx and/or interferes with phospholamban

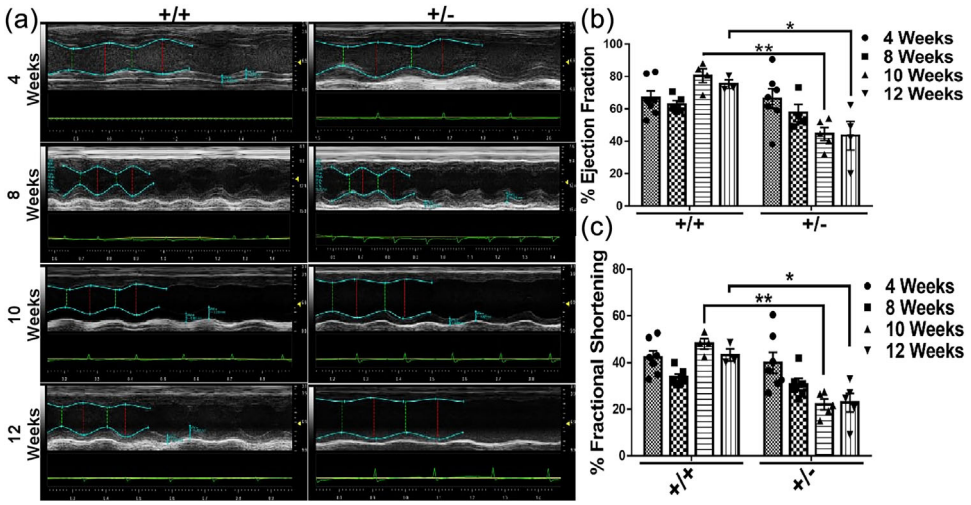

FIGURE 2 Effects of BAG3 Haplo-insufficiency on cardiac function. (a) Representative M-mode echocardiograms of cBAG3$^{+/+}$ and cBAG3$^{+/-}$ mice at 4, 8, 10, and 12 weeks of age. (b & c) Quantification of ejection fraction (b) and percent fractional shortening (c) at 4, 8, 10, and 12 weeks of age. For cBAG3$^{+/+}$ mice n = 10, 6, 4 and 3 at each time point respectively and for cBAG3$^{+/-}$ mice n = 8, 6, 5, and 4 at each time point respectively. $^{**}p < 0.0001$, $^{*}p = 0.0004$

TABLE 1 Contractility and calcium handling in isolated myocytes from cBAG3$^{+/+}$ and cBAG3$^{+/-}$ mice.

	Percent cell length	Percent cell length with ISO
cBAG3$^{+/+}$	4.96 ± 0.16 (15)	11.86 ± 0.41 (11)
cBAG3$^{+/-}$	4.95 ± 0.27 (16) (NS)	10.66 ± 0.35 (14)***
	Systolic $[Ca^{2+}]_i$ (nM)	Systolic $[Ca^{2+}]_i$ (nM) With ISO
cBAG3$^{+/+}$	215 ± 14 (11)	633 ± 43 (15)
cBAG3$^{+/-}$	202 ±n11 (16) (NS)	428 ± 28 (12)***
	Diastolic $[Ca^{2+}]_i$ (nM)	Diastoic $[Ca^{2+}]_i$ (nM) With ISO
cBAG3$^{+/+}$	96 ± 7 (11)	91 ± 7 (15)
cBAG3$^{+/-}$	98 ± 7 (16) (NS)	94 ± 6 (12)
	Transient amplitude (%)	Transient amplitude (%) with ISO
cBAG3$^{+/+}$	18.6 ± 1.2 (11)	58.6 ± 2.5 (15)
cBAG3$^{+/-}$	17.9 ± 1.0 (16) (NS)	46.2 ± 2.2 (12)**

Units of [Ca2+]iI transient amplitude: % increase of fura intensity ratio. Contractility and Ca^{2+} handling were not different at baseline (NS) but were reduced in the presence of isoproterenol (ISO). n = number of cells in 3 separate preparations; values are mean ± SE; $^{***}p < 0.0001$. $^{**}p = 0.001$.

phosphorylation, thereby limiting Ca^{2+} uptake into the sarcoplasmic reticulum.

3.4 | Both apoptosis and autophagy are dysregulated in BAG3 deficient mice

As seen in Figure 3a and 3b, adult myocytes isolated from either cBAG3$^{+/-}$ or cBAG3$^{+/+}$ mice and transfected with the autophagy flux reporter construct Adv-RFP-GFP-LC3 demonstrated similar amounts of LC3 puncta at baseline. However, inclusion of Bafilomycin A1 in the culture media did not result in an increase in the number of LC3 puncta in adult myocytes isolated from cBAG3$^{+/-}$ hearts. By contrast, there was a significant increase in LC3 puncta in myocytes isolated from cBAG3$^{+/+}$ when Bafilomycin A1 was included in the culture media suggesting that BAG3 haplo-insufficiency is associated with a significant decrease in autophagy flux ($p < 0.04$). Consistent with the decrease in LC3 puncta in myocytes from cBAG3$^{+/-}$ mice infected with the Adv-RFP-GFP reporter gene, we also failed to find an increase in LC3I and II in adult myocytes from cBAG3$^{+/-}$ mice that had been incubated with Bafilomycin A1 when compared with the obvious increase in LC3I and II seen in myocytes isolated from cBAG3$^{+/+}$ hearts (Figure 4).

Similar to the effects on autophagy, BAG3 haplo-insufficiency was associated with a significant increase in apoptosis. As seen in Figure 3C and 3D, the number of apoptotic cells increased significantly ($p < 0.0001$) in myocytes isolated from cBAG3$^{+/-}$ mice when compared with cBAG3$^{+/+}$ controls. In fact, less than 8% of the total cells from the

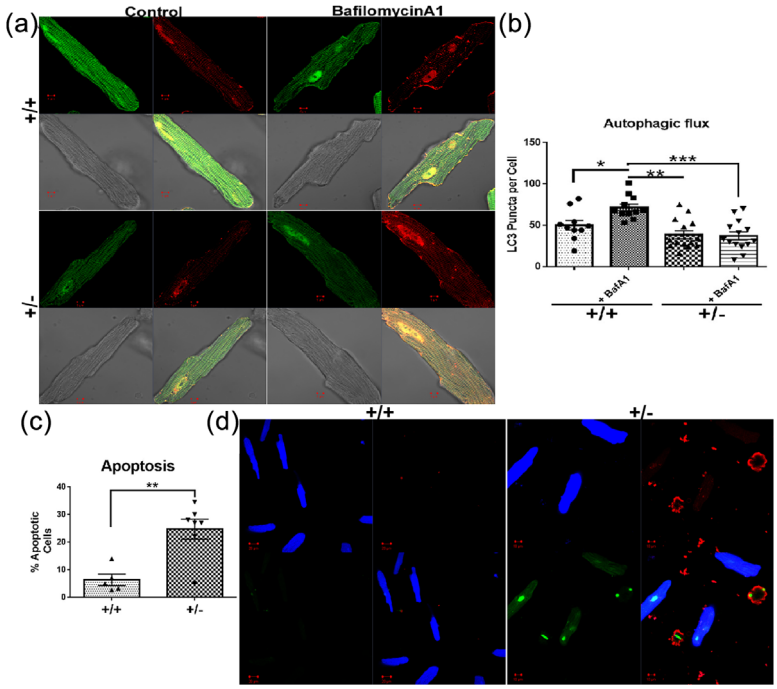

FIGURE 3 Effects of BAG3 haplo-insufficiency on autophagy and apoptosis. (a) Representative confocal images of isolated adult cardiomyocytes from both cBAG3$^{+/+}$ and cBAG3$^{+/-}$ mice infected with Ad-GFP-RFP-LC3 reporter construct with and without treatment with Bafilomycin A1. (B) Quantification of LC3 puncta per cell. *n* = at least 9 cells from 3 separate isolations. **p* = 0.03, ***p* = 0.007, ****p* < 0.0001. (c) Quantification of percent apoptotic cells per field in cBAG3$^{+/+}$ and cBAG3$^{+/-}$ cardiomyocytes. *n* = at least 10 fields from three separate isolations. p = 0.006. (D) Representative confocal images of cBAG3$^{+/+}$ and cBAG3$^{+/-}$ stained for phosphatidylserine (red), compromised nuclei (green) and a cytoplasm dye for viable cells (blue)

control mice stained for the apoptosis marker whereas programmed cell death was detected in 24% of the cells isolated from the cBAG3$^{+/-}$ mice with BAG3 haplo-insufficiency.

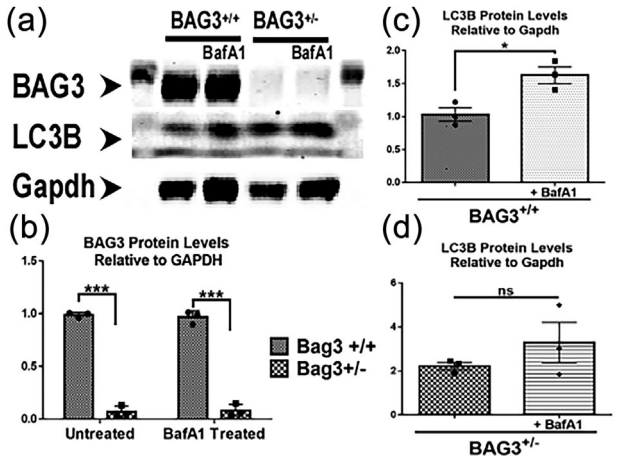

FIGURE 4 Effects of BAG3 haplo-insufficiency on autophagy flux. (a) Representative blot of BAG3, LC3, and GAPDH from cardiac myocytes isolated from cBAG3$^{+/+}$ and cBAG3$^{+/-}$ mice with and without treatment with bafilomycin A1. (b) Quantification of BAG3 levels as measured by western blotting when normalized to GAPDH. (c) Quantification of LC3I and LC3II in BAG3$^{+/+}$ myocytes when normalized to GAPDH. (d) Quantification of LC3I and LC3II in cBAG3$^{+/-}$ myocytes when normalized to GAPDH. Each experiment was repeated three times. n = 3 for all conditions. ****p* < 0.0001; **p* = 0,0006

4 | DISCUSSION

The BAG3 gene is increasingly being recognized as an important dilated cardiomyopathy locus (Franaszczyk et al., 2014). However, the mechanisms responsible for the development of the LV dysfunction phenotype have been elusive because of the absence of readily available animal models in which to study the biology of BAG3. Therefore, we used BAG3 single allele floxed (BAG3$^{fl/+}$) mice and αMHC-Cre mice (Agah et al., 1997) to generate the first mouse with heterozygous constitutive and cardiac-restricted BAG3 knockdown. The mice showed haplo-insufficiency of BAG3, diminished responsiveness to β-adrenergic stimulation, a modest but significant decrease in autophagy flux and a robust increase in apoptosis. The biologic phenotype of the cBAG3$^{+/-}$ mouse is consistent with our previous observations in mice with left ventricular dysfunction after a myocardial infarction (Knezevic et al., 2016), in mice after ischemia/reperfusion (Su et al., 2016) and in isolated adult myocytes in which BAG3 is knocked-down with an siRNA – all of which demonstrate an approximately 50% reduction in BAG3 levels (Feldman et al., 2016). Thus, the available data suggests that cBAG3$^{+/-}$ mice can provide a useful model for studying the biology of BAG3 mutations that result in haplo-insufficiency.

It is notable that the phenotype of the cBAG3$^{+/-}$ mouse is disparate from recent reports of mice in which BAG3 was knocked out globally or that have a homozygous BAG3 loss-of-function mutation. For example, Homma et al first reported that homozygous deletion of BAG3 led to

catastrophic myofibrillar disruption with death by 4 weeks of age; however, mice with heterozygous BAG3 disruption had a normal phenotype (Homma et al., 2006). We too found a normal phenotype in mice with haplo-insufficiency of BAG3 at 4 weeks of age; however, by 10 weeks of age they began to demonstrate a significant reduction in LV function. Importantly, young cBAG3$^{+/-}$ mice have significant LV dysfunction in the absence of significant dilatation or hypertrophy, a phenotype that is remarkably different from the profound chamber dilation seen in mice after a myocardial infarction and the marked hypertrophy seen after trans-aortic constriction. Thus these mice provide an interesting window into the early stages of LV dysfunction.

Fang et al. (2017) recently showed that cardiac-restricted BAG3-KO and Glu455Lys-knockin led to the development of a dilated cardiomyopathy due to decreased binding to HSP70 and a subsequent decrease in autophagy flux. They also showed that decreased coupling with HSP70 in both BAG3-KO and Glu455Lys mice was responsible in part for the phenotype. BAG3-KO also decreased contractility but not $[Ca^{2+}]_I$ transient amplitudes in single myocytes. By contrast, we found that 10 week old cBAG3$^{+/-}$ myocytes had normal contractility and Ca^{2+} amplitudes at rest − but diminished contractility and $[Ca^{2+}]_I$ transient amplitudes in response to isoproterenol. Furthermore, while the reduction in autophagy flux found in cBAG3$^{+/-}$ mice was modest, there was a robust increase in apoptosis that was not observed by Fang et al. Thus, cBAG3$^{+/-}$ mice demonstrate a phenotype that accurately mirrors the phenotype seen in individuals with haplo-insufficiency yet differs from the phenotype seen with homozygosity.

Our results provide several important clues regarding the pathobiology of reduced levels of BAG3. First, they support the hypothesis that genetic variants resulting in a loss of BAG3 from a single allele can lead to diminished left ventricular function. Second, the present study demonstrates that a BAG3 variant on a single allele has multiple adverse effects on the heart including decreased b-adrenergic responsiveness, diminished autophagy flux and increased apoptosis and these adverse effects can be seen even early in the course of disease before the ventricle has dilated. In aggregate, these results suggest that cBAG3$^{+/-}$ mice can serve as a useful model for mechanistic studies directed at understanding the molecular and cellular regulation of BAG3 in the heart.

ACKNOWLEDGMENTS

This work was supported by the National Institutes of Health grants: RO1-HL123093 (JG & KK) RO1-HL58672, RO1-HL74854 and RO1-HL123-93 (JYC) and PO1-HL91799 (Project 2) and RO1-HL123093 (AMF).

CONFLICT OF INTEREST

Ms Myers and Drs. Feldman, Cheung, McClung and Kontos are founders of and own shares in Renovacor, Inc., a start-up company developing therapeutics that target BAG3. All other authors have reported that they have no relationships relevant to the content of this paper to disclose.

ORCID

Arthur M. Feldman http://orcid.org/0000-0001-8351-9569

REFERENCES

Agah, R., Frenkel, P. A., French, B. A., Michael, L. H., Overbeek, P. A., & Schneider, M. D. (1997). Gene recombination in postmitotic cells. Targeted expression of cre recombinase provokes cardiac-restricted, site-specific rearrangement in adult ventricular muscle in vivo. *The Journal of Clinical Investigation*, *100*, 169–179.

Arimura, T., Ishikawa, T., Nunoda, S., Kawai, S., & Kimura, A. (2011). Dilated cardiomyopathy-associated BAG3 mutations impair Z-disc assembly and enhance sensitivity to apoptosis in cardiomyocytes. *Human Mutation*, *32*, 1481–1491.

Behl, C. (2016). Breaking BAG: The co-chaperone BAG3 in health and disease. *Trends in Pharmacological Sciences*, *37*, 672–688.

Bradley, A., Anastassiadis, K., Ayadi, A., Battey, J. F., Bell, C., Birling, M. C., … Wurst, W. (2012). The mammalian gene function resource: The international knockout mouse consortium. *Mammalian Genome*, *23*, 580–586.

Capasso, S., Alessio, N., Squillaro, T., Di Bernardo, G., Melone, M. A., Cipollaro, M., … Galderisi, U. (2015). Changes in autophagy, proteasome activity and metabolism to determine a specific signature for acute and chronic senescent mesenchymal stromal cells. *Oncotarget*, *6*, 39457–39468.

Chami, N., Tadros, R., Lemarbre, F., Lo, K. S., Beaudoin, M., Robb, L., … Lettre, G. (2014). Nonsense mutations in BAG3 are associated with early-onset dilated cardiomyopathy in French Canadians. *Canadian Journal of Cardiology*, *30*, 1655–1661.

Fang, X., Bogomolovas, J., Wu, T., Zhang, W., Liu, C., Veevers, J., … Chen, J. (2017). Loss-of-function mutations in co-chaperone BAG3 destabilize small HSPs and cause cardiomyopathy. *The Journal of Clinical Investigation*, *127*, 3189–3200.

Feldman, A. M., Begay, R. L., Knezevic, T., Myers, V. D., Slavov, D. B., Zhu, W., … Taylor, M. R. (2014). Decreased levels of BAG3 in a family with a rare variant and in idiopathic dilated cardiomyopathy. *Journal of Cellular Physiology*, *229*, 1697–1702.

Feldman, A. M., Gordon, J., Wang, J., Song, J., Zhang, X. Q., Myers, V. D., … Cheung, J. Y. (2016). BAG3 regulates contractility and Ca(2 +) homeostasis in adult mouse ventricular myocytes. *Journal of Molecular and Cellular Cardiology*, *92*, 10–20.

Franaszczyk, M., Bilinska, Z. T., Sobieszczanska-Malek, M., Michalak, E., Sleszycka, J., Sioma, A., … Ploski, R. (2014). The BAG3 gene variants in polish patients with dilated cardiomyopathy: Four novel mutations and a genotype-phenotype correlation. *Journal of Translational Medicine*, *12*, 192.

Homma, S., Iwasaki, M., Shelton, G. D., Engvall, E., Reed, J. C., & Takayama, S. (2006). BAG3 deficiency results in fulminant myopathy and early lethality. *The American Journal of Pathology*, *169*, 761–773.

Klionsky, D. J., Abdelmohsen, K., Abe, A., Abedin, M. J., Abeliovich, H., Acevedo Arozena, A., … Zughaier, S. M. (2016). Guidelines for the use and interpretation of assays for monitoring autophagy (3rd edition). *Autophagy*, *12*, 1–222.

Knezevic, T., Myers, V. D., Su, F., Wang, J., Soong, J., Zhang, X. Q., … Feldman, A. M. (2016). Adeno-associated virus serotype 9 − driven expression of BAG3 significantly improves left ventricular function in murine hearts with left ventricular dysfunction secondary to a myocardial infarction. *JACC Basic Translation Science*, *1*, 646–653.

Ma, X., Liu, H., Foyil, S. R., Godar, R. J., Weinheimer, C. J., Hill, J. A., & Diwan, A. (2012). Impaired autophagosome clearance contributes to cardiomyocyte death in ischemia/reperfusion injury. *Circulation*, *125*, 3170–3181.

Norton, N., Li, D., Rieder, M. J., Siegfried, J. D., Rampersaud, E., Zuchner, S., ... Hershberger, R. E. (2011). Genome-wide studies of copy number variation and exome sequencing identify rare variants in BAG3 as a cause of dilated cardiomyopathy. *American Journal of Human Genetics*, *88*, 273–282.

Pettitt, S. J., Liang, Q., Rairdan, X. Y., Moran, J. L., Prosser, H. M., Beier, D. R., ... Skarnes, W. C. (2009). Agouti C57BL/6N embryonic stem cells for mouse genetic resources. *Nature Methods*, *6*, 493–495.

Selcen, D., Muntoni, F., Burton, B. K., Pegoraro, E., Sewry, C., Bite, A. V., & Engel, A. G. (2009). Mutation in BAG3 causes severe dominant childhood muscular dystrophy. *Annals of Neurology*, *65*, 83–89.

Skarnes, W. C., Rosen, B., West, A. P., Koutsourakis, M., Bushell, W., Iyer, V., ... Bradley, A. (2011). A conditional knockout resource for the genome-wide study of mouse gene function. *Nature*, *474*, 337–342.

Song, J., Gao, E., Wang, J., Zhang, X. Q., Chan, T. O., Koch, W. J., ... Cheung, J. Y. (2012). Constitutive overexpression of phosphomimetic phospholemman S68E mutant results in arrhythmias, early mortality, and heart failure: Potential involvement of Na+/Ca2+ exchanger. *American Journal of Physiology-Heart and Circulatory Physiology*, *302*, H770–H781.

Song, J., Zhang, X. Q., Wang, J., Cheskis, E., Chan, T. O., Feldman, A. M., ... Cheung, J. Y. (2008). Regulation of cardiac myocyte contractility by phospholemman: Na+/Ca2+ exchange versus Na+ −K+ −ATPase. *American Journal of Physiology-Heart and Circulatory Physiology*, *295*, H1615–H1625.

Su, F., Myers, V. D., Knezevic, T., Wang, J., Gao, E., Madesh, M., ... Feldman, A. M. (2016). Bcl-2-associated athanogene 3 protects the heart from ischemia/reperfusion injury. *Journal of Clinical Investigation Insight*, *1*, 90931.

Tanida, I., Ueno, T., & Kominami, E. (2008). LC3 and autophagy. *Methods in Molecular Biology*, *445*, 77–88.

Tilley, D. G., Zhu, W., Myers, V. D., Barr, L. A., Gao, E., Li, X., ... Feldman, A. M. (2014). Beta-adrenergic receptor-mediated cardiac contractility is inhibited via vasopressin type 1A-receptor-dependent signaling. *Circulation*, *130*, 1800–1811.

Toro, R., Perez-Serra, A., Campuzano, O., Moncayo-Arlandi, J., Allegue, C., Iglesias, A., ... Brugada, R. (2016). Familial dilated cardiomyopathy caused by a novel frameshift in the BAG3 gene. *PLoS ONE*, *11*, 0158730.

Tucker, A. L., Song, J., Zhang, X. Q., Wang, J., Ahlers, B. A., Carl, L. L., ... Cheung, J. Y. (2006). Altered contractility and [Ca2+]i homeostasis in phospholemman-deficient murine myocytes: Role of Na+/Ca2+ exchange. *American Journal of Physiology-Heart and Circulatory Physiology*, *291*, H2199–H2209.

Villard, E., Perret, C., Gary, F., Proust, C., Dilanian, G., Hengstenberg, C., ... Cambien, F. (2011). A genome-wide association study identifies two loci associated with heart failure due to dilated cardiomyopathy. *European Heart Journal*, *32*, 1065–1076.

Wang, J., Chan, T. O., Zhang, X. Q., Gao, E., Song, J., Koch, W. J., ... Cheung, J. Y. (2009). Induced overexpression of Na+/Ca2+ exchanger transgene: Altered myocyte contractility, [Ca2 +]i transients, SR Ca2+ contents, and action potential duration. *American Journal of Physiology-Heart and Circulatory Physiology*, *297*, H590–H601.

Wang, J., Gao, E., Rabinowitz, J., Song, J., Zhang, X. Q., Koch, W. J., ... Cheung, J. Y. (2011). Regulation of in vivo cardiac contractility by phospholemman: Role of Na+/Ca2+ exchange. *American Journal of Physiology-Heart and Circulatory Physiology*, *300*, H859–H868.

Wang, J., Gao, E., Song, J., Zhang, X. Q., Li, J., Koch, W. J., ... Cheung, J. Y. (2010). Phospholemman and beta-adrenergic stimulation in the heart. *American Journal of Physiology-Heart and Circulatory Physiology*, *298*, H807–H815.

Zhou, Y. Y., Wang, S. Q., Zhu, W. Z., Chruscinski, A., Kobilka, B. K., Ziman, B., ... Xiao, R. P. (2000). Culture and adenoviral infection of adult mouse cardiac myocytes: Methods for cellular genetic physiology. *American Journal of Physiology-Heart and Circulatory Physiology*, *279*, H429–H436.

How to cite this article: Myers VD, Tomar D, Madesh M, et al. Haplo-insufficiency of Bcl2-associated athanogene 3 in mice results in progressive left ventricular dysfunction, β-adrenergic insensitivity, and increased apoptosis. *J Cell Physiol*. 2018;233:6319–6326. https://doi.org/10.1002/jcp.26482